

Conic Epipolar Constraints from Affine Correspondences

Jacob Bentolila^a, and Joseph M. Francos^b

^a*Ben Gurion University
Electrical & Computer Engineering Department
P.O.B 653 Beer-Sheva 84105, Israel
bentolil@ee.bgu.ac.il*

^b*Ben Gurion University
Electrical & Computer Engineering Department
P.O.B 653 Beer-Sheva 84105, Israel
francos@ee.bgu.ac.il*

Abstract

We derive an explicit relation between local affine approximations resulting from matching of affine invariant regions and the epipolar geometry in the case of a two view geometry. Most methods that employ the affine relations do so indirectly by generating pointwise correspondences from the affine relations. In this paper we derive an explicit relation between the local affine approximations and the epipolar geometry.

We show that each affine approximation between images is equivalent to three linear constraints on the fundamental matrix and that the linear conditions guarantee the existence of an homography, compatible with the fundamental matrix. We further show that two affine relations constrain the location of the epipole to a conic section. Therefore, the location of the epipole can be extracted from 3 regions by intersecting conics.

The result is further employed to derive a procedure for estimating the fundamental matrix, based on the estimated location of the epipole. It is

shown to be more accurate and to require less iterations in LO-RANSAC based estimation, than the current point based approaches that employ the affine relation to generate pointwise correspondences and then calculate the fundamental matrix from the pointwise relations.

Keywords: epipolar geometry, affine invariant regions, fundamental matrix, homographies

1. Introduction

Solving the geometry of a stereo rig is a preliminary step in solving many problems in computer vision such as image registration, structure from motion and object tracking. Luong and Faugeras [1] showed in 1995 that the geometry of two uncalibrated cameras can be described by a 3×3 singular matrix called the fundamental matrix. The fundamental matrix provides the correspondence between points in each image to lines in the other image and therefore greatly simplifies the task of finding correspondence points between images. Furthermore, once the fundamental matrix is known, a correspondence of points between the images allows for reconstruction of a 3D scene up to a projection ambiguity [2].

The fundamental matrix can be estimated from correspondence of points between two images [3]. Each point correspondence yields a linear constraint on the location of the epipole; since the matrix is only determined up to scale, a correspondence of 8 points [4] results in a linear estimation of the matrix. An estimation of the fundamental matrix based on a correspondence of 7 points can be calculated by exploiting the singularity of the matrix [2]. It was further shown by Faugeras [5] that a correspondence of 6 points limits

the location of the epipole to a 3rd order rational curve.

In recent years, several methods have been proposed for matching of small regions between images [6],[7],[8],[9]. Region correspondence methods usually assume that the geometric deformation between the images can be approximated locally by an affine transformation. Furthermore, affine normalization of the regions provides an approximation of a point correspondence and the local derivatives of the deformation between the images at the point of the correspondence [10]. We denote such a correspondence of points along with the derivatives of the deformation between the images at the point of correspondence by the name *affine correspondence*.

The additional information available in the affine correspondence is rarely used for the calculation of the fundamental matrix. Methods that do employ information from affine correspondences try to convert the affine correspondence into point correspondences. Generally, since an affine transformation is determined by 3 points, it seems that it is roughly equivalent to the matching of 3 points between images. In [11],[12],[13],[14] local affine approximation is used for generation of additional points. However, affine correspondences and point correspondences are different mathematical entities; there is no equivalence between an affine correspondence and a certain number of point correspondences. For example, 4 points of correspondence between images fully determine an homography between the images [2] whereas an affine correspondence and a single point correspondence do not fully determine an homography (we show in Section 3 that the direction of the transformation of an arbitrary point by an homography relative to the center of the affine correspondence is known from the affine correspondence. Therefore, the point

correspondence only contributes a single constraint instead of two).

A non pointwise approach for calculating an affine fundamental matrix was presented in [15]. The method treats the affine correspondences as matched ellipses between the two images. It is shown that matching of two ellipses between images is sufficient for calculation of an affine fundamental matrix. However, the affine fundamental matrix has only 4 degrees of freedom as opposed to 7 in a general fundamental matrix. Such a model assumes that the camera centers are at infinity; it is therefore more suitable for narrow field of view cameras. Furthermore, notice that one degree of freedom is discarded from the affine correspondence as matched ellipses only determine an affine correspondence up to a rotation factor [10].

To the best of our knowledge, there is no theoretical work that derives explicit constraints from affine correspondences on the epipolar geometry. In this paper, we offer a different point of view on the relation between affine correspondences and the epipolar geometry. We treat the affine correspondence as the derivative of an homography caused by a plane tangent to the surface viewed by the two cameras at the point of correspondence. The compatibility requirement between an homography and a fundamental matrix [2] is then employed for deriving constraints on the fundamental matrix. We prove that an affine correspondence yields 3 linear constraints on the fundamental matrix; we further prove that the linear constraints are sufficient conditions for an homography compatible with the fundamental matrix to exist. Therefore, 3 affine correspondences are sufficient to fully determine the fundamental matrix.

In the case where two affine correspondences are known, a one dimensional

family of solutions exists; we show that in this case the location of the epipole is constrained to a conic. We employ the result to calculate the location of the epipole from 3 pairs of affine correspondences by intersection of conics. The proposed method shows an improvement of up to an order of magnitude in the accuracy of estimating the fundamental matrix over using 3 points from each region with the traditional normalized 8 points algorithm. We also employ the proposed method for calculation of the fundamental matrix from matching hypotheses with low inliers rate by using Locally Optimized RANSAC [16]. In such cases the proposed methods showed comparable and slightly better results than the state of the art, point based, method [11].

2. Constraints on the Fundamental Matrix from an Affine Correspondence

A surface viewed by a pair of cameras induces a set of correspondence points between the viewed images. An affine correspondence $(\mathbf{u}_0, \mathbf{u}'_0, A_0)$ between a pair of images is a pair of corresponding pixel coordinates $(\mathbf{u}_0, \mathbf{u}'_0)$ along with the local derivatives at the point of correspondence, $A_0 = \frac{d\mathbf{u}'}{d\mathbf{u}}|_{\mathbf{u}_0}$. The matrix A_0 may be regarded as the Jacobian matrix of the homography that represents the point correspondence on a 3D plane, tangent to the viewed surface at the correspondence point (see Figure 1).

An homography, H , is said to be compatible with a fundamental matrix, F , if and only if $H^T F$ is an anti-symmetric matrix [2]. Therefore, a known homography between a pair of images yields 6 linear constraints on the fundamental matrix. However, an affine correspondence does not fully determine an homography. In Section 2.2 we wish to determine the constraints on the

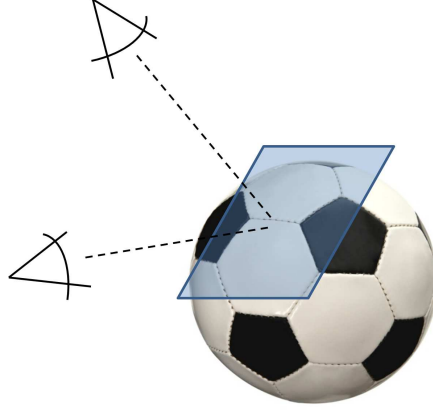


Figure 1: An affine correspondence as the derivatives of an homography. The homography represents the correspondence between two cameras along the tangent plane of the viewed surface (at the point of correspondence); the affine correspondence consists of the point of correspondence along with the derivatives of the homography at the correspondence point.

fundamental matrix resulting from an homography which is not fully known, as only the affine correspondence $(\mathbf{u}_0, \mathbf{u}'_0, A_0)$ is known.

2.1. Homography as an affine correspondence with 2 unknown terms

Let H be an homography that represents the image correspondence caused by a world plane viewed in a pair of images; also let $(\mathbf{u}_0, \mathbf{u}'_0, A)$ be an affine correspondence between the images of the world plane. As shown next, the affine correspondence determines the terms of an homography H up to two unknowns terms. We denote the terms of A as

$$A = \begin{pmatrix} a_1 & a_3 \\ a_2 & a_4 \end{pmatrix} \quad (1)$$

and the terms of the homography H , expanded in homogeneous coordinates, as

$$H = \begin{pmatrix} h_1 & h_4 & h_7 \\ h_2 & h_5 & h_8 \\ h_3 & h_6 & h_9 \end{pmatrix} \quad (2)$$

The relation between H and A is expressed by the derivatives of the homography H at \mathbf{u}_0 . Let u_x and u_y represent the first and second coordinates of \mathbf{u} ($\mathbf{u} = (u_x, u_y)^T$) and \mathbf{u}' the transformation of u by H . The derivative $\frac{du'_x}{du_x}|_{u_0}$ is expressed as

$$\frac{d}{du_x} \left(\frac{h_1 u_x + h_4 u_y + h_7}{h_3 u_x + h_6 u_y + h_9} \right) \Big|_{u_0} = \frac{h_1(h_3 u_{0,x} + h_6 u_{0,y} + h_9) + h_3(h_1 u_{0,x} + h_4 u_{0,y} + h_7)}{(h_3 u_{0,x} + h_6 u_{0,y} + h_9)^2} \quad (3)$$

We limit the discussion to the case where $\mathbf{u}_0 = 0$ and $\mathbf{u}'_0 = 0$ (The general case can be reduced to this case by a shift of coordinates). Since $\mathbf{u}_0 = \mathbf{0}$ and $\mathbf{u}'_0 = \mathbf{0}$ then, using (2), $h_7 = h_8 = 0$ and, using (1) we have

$$a_1 = \frac{du'_x}{du_x} \Big|_{u_0} = \frac{h_1}{h_9} \quad (4)$$

A similar calculation relates a_2, a_3, a_4 to h_2, h_4, h_5 respectively. Since the matrix H is only determined up to a scale factor, we can set $h_9 = 1$, therefore H takes the form

$$H = \begin{pmatrix} a_1 & a_3 & 0 \\ a_2 & a_4 & 0 \\ h_3 & h_6 & 1 \end{pmatrix} \quad (5)$$

leaving only 2 unknown parameters. In the general case where $\mathbf{u}_0 \neq 0$ and $\mathbf{u}'_0 \neq 0$ the same relation applies after shifting the coordinates systems. Let

$S_{\mathbf{u}}$ be a shift of the coordinates system:

$$S_{\mathbf{u}} = \begin{pmatrix} 1 & 0 & u_x \\ 0 & 1 & u_y \\ 0 & 0 & 1 \end{pmatrix} \quad (6)$$

The homography in this case is achieved by shifting (5):

$$H = S_{\mathbf{u}'_0} \begin{pmatrix} a_1 & a_3 & 0 \\ a_2 & a_4 & 0 \\ h_3 & h_6 & 1 \end{pmatrix} S_{-\mathbf{u}_0} \quad (7)$$

We conclude that $\mathbf{u}_0, \mathbf{u}'_0$ and A explicitly determine the form of an homography, leaving two undetermined degrees of freedom.

2.2. Constraints on the fundamental matrix from affine correspondences

As previously mentioned, an homography forms 6 linear constraints on the elements of the fundamental matrix. If only an affine correspondence is known, the 6 equations contain two parameters, h_3 and h_6 , that describe the unknown terms of the homography. We show next that the 6 equations are equivalent to 3 linear equations on F and one polynomial equation.

The derivation is performed for the case where $\mathbf{u}_0 = \mathbf{u}'_0 = 0$ (As mentioned before, the general case can be reduced to this case by shifting the coordinate system). By (5) the anti-symmetric requirement on $H^T F$ results

in 6 equations:

$$f_9 = 0 \quad (8)$$

$$f_6 + a_3 f_7 + a_4 f_8 + h_6 f_9 = 0 \quad (9)$$

$$f_3 + a_1 f_7 + a_2 f_8 + h_3 f_9 = 0 \quad (10)$$

$$a_3 f_4 + a_4 f_5 + h_6 f_6 = 0 \quad (11)$$

$$a_1 f_1 + a_2 f_2 + h_3 f_3 = 0 \quad (12)$$

$$a_1 f_4 + a_2 f_5 + h_3 f_6 + a_3 f_1 + a_4 f_2 + h_6 f_3 = 0 \quad (13)$$

Substituting (8) to (9) and (10), the non linear terms vanish. Therefore, three linear equations are formed. The linear equations can be simply formulated as

$$f_9 = 0 \quad (14)$$

$$\begin{pmatrix} f_3 \\ f_6 \end{pmatrix} = -A^T \begin{pmatrix} f_7 \\ f_8 \end{pmatrix} \quad (15)$$

An homography H , compliant with a fundamental matrix F , must also satisfy the non linear equations (11)-(13). Note that h_3 and h_6 in (11) and (12) can be expressed as rational functions of the terms of F . They can therefore be substituted into equation (13) to yield

$$\begin{aligned} a_1 f_4 + a_2 f_5 + a_3 f_1 + a_4 f_2 - \frac{f_6}{f_3}(a_1 f_1 + a_2 f_2) \\ - \frac{f_3}{f_6}(a_3 f_4 + a_4 f_5) = 0 \end{aligned} \quad (16)$$

The rational equation can be expressed in a polynomial form by multiplying

(16) by $f_3 f_6$:

$$\begin{aligned} f_3 f_6 (a_1 f_4 + a_2 f_5 + a_3 f_1 + a_4 f_2) - (f_6)^2 (a_1 f_1 + a_2 f_2) \\ - (f_3)^2 (a_3 f_4 + a_4 f_5) = 0 \end{aligned} \quad (17)$$

Equations (11)-(13) therefore result in a single third order polynomial equation in the terms of F .

Since by definition $\det(F) = 0$, we next show that (17) is in fact redundant. Given a non singular homography matrix H , the anti-symmetric requirement imposed at the beginning of our derivation also implies that $\det(H^T F) = 0$ and therefore $\det(F) = 0$. The requirement that $\det(F) = 0$ forms a third order polynomial equation in the terms of F . Therefore, any solution of (17) must result a singular F . Indeed, by substituting (14)-(15) into (17), equation (17) can be rewritten in the form

$$\det(A)\det(F) = 0 \quad (18)$$

Again, since A is invertible, a solution only exists if $\det(F) = 0$. This is however a general property of the fundamental matrix as all fundamental matrices are singular. Therefore, the linear equations (14)-(15) are sufficient to guarantee the existence of an homography, H , with derivatives A at \mathbf{u}_0 and a fundamental matrix F that is compatible with H . To conclude, each affine correspondence results in 3 linear equations on the terms on the fundamental matrix F . Moreover, an homography, compatible with a fundamental matrix can always be calculated from an affine correspondence if the linear constraints (14)-(15) are met.

3. Deriving an Epipolar Constraint from a Pair of Affine Correspondences

As a result of the previous section, the fundamental matrix cannot be fully determined by a pair of affine correspondences: The fundamental matrix has 7 degrees of freedom. Since each affine correspondence yields 3 linear equations on the fundamental matrix, a pair of affine correspondences should result in a one dimensional family of solutions to the fundamental matrix. It was shown by Faugeras [5] that 6 *points* of correspondence constrain the location of the epipole to a cubic. An interesting question is: What does a pair of affine correspondences tell us about the geometry of the corresponding image pairs? In this section, we show that 2 affine correspondences constrain the location of the epipole to a second order rational curve.

Let $(\mathbf{u}_1, \mathbf{u}'_1, A_1)$ and $(\mathbf{u}_2, \mathbf{u}'_2, A_2)$ denote two affine correspondences. As shown in Section 2, each affine correspondence may be expressed through the derivatives of an homography at the specific point of correspondence. We denote the homographies as H_1 and H_2 . The line connecting \mathbf{u}_1 and \mathbf{u}_2 plays an important role in the derivation of the epipolar constraint presented here; we denote the transformations of the vector $\mathbf{u}_1 - \mathbf{u}_2$ by A_1 and A_2 as $\mathbf{v}_1 = A_1(\mathbf{u}_1 - \mathbf{u}_2)$ and $\mathbf{v}_2 = A_2(\mathbf{u}_1 - \mathbf{u}_2)$.

We denote a general point on the line connecting \mathbf{u}_1 and \mathbf{u}_2 as

$$\mathbf{x}(\beta) = \mathbf{u}_1 + \beta(\mathbf{u}_1 - \mathbf{u}_2) \tag{19}$$

A transformation of $\mathbf{x}(\beta)$ by H_1 and H_2 to the points $\mathbf{x}'^{(1)}(\beta)$ and $\mathbf{x}'^{(2)}(\beta)$ respectively, yields a linear constraint on the epipole location as by the definition of the epipolar line the epipole and the two points should be collinear

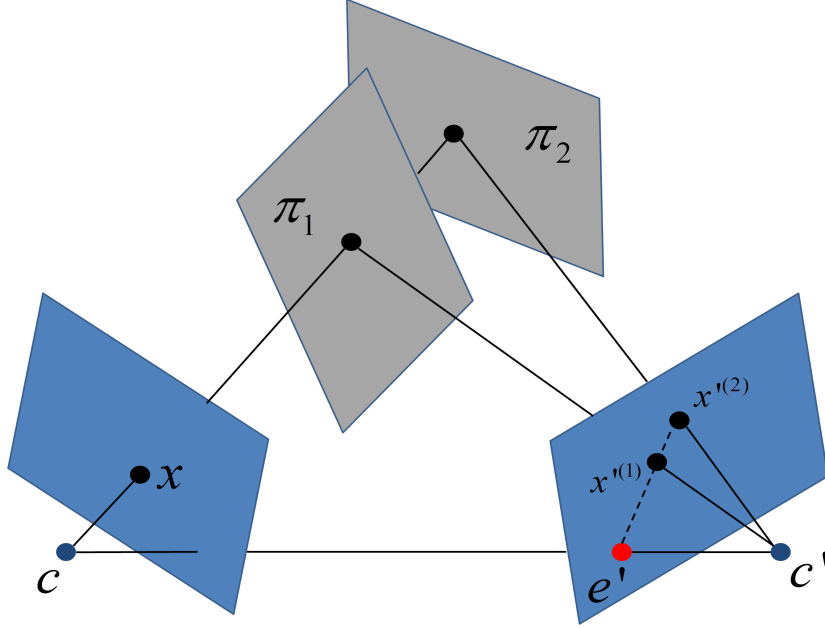


Figure 2: An illustration of the epipolar line constraint from a point \mathbf{x} transformed by two homographies H_1 and H_2 to the points $\mathbf{x}'^{(1)}$ and $\mathbf{x}'^{(2)}$ respectively. An homography H_i represents the correspondence of points on a world plane π_i in the two cameras. The line connecting $\mathbf{x}'^{(1)}$ and $\mathbf{x}'^{(2)}$ is an epipolar line of the camera C'

(see Figure 2). The epipolar line connecting $\mathbf{x}'^{(1)}(\beta)$ and $\mathbf{x}'^{(2)}(\beta)$ can therefore be formalized as

$$\mathbf{l}(\beta) = \begin{pmatrix} \mathbf{x}'^{(1)}(\beta) \\ 1 \end{pmatrix} \times \begin{pmatrix} \mathbf{x}'^{(2)}(\beta) \\ 1 \end{pmatrix} \quad (20)$$

and the location of the epipole, \mathbf{e} , obeys the rule $\mathbf{e}^T \mathbf{l}(\beta) = 0$.

Equation (20) forms a pointwise constraint on the location of the epipole. Since an affine correspondence also consists of derivatives we wish to exploit the derivatives to further constrain the location of the epipole. A second line is therefore generated by relating infinitesimal movements of $\mathbf{x}'^{(1)}(\beta)$ and $\mathbf{x}'^{(2)}(\beta)$ caused by an infinitesimal movement of $\mathbf{x}(\beta)$. The configuration is

illustrated in Figure 3. Since the epipole location does not depend on β , the infinitesimal relation is formalized by taking the derivative of $\mathbf{e}^T \mathbf{l}(\beta) = 0$. Therefore, $\mathbf{e}^T \frac{d\mathbf{l}}{d\beta}(\beta) = 0$ where

$$\frac{d\mathbf{l}}{d\beta}(\beta) = \begin{pmatrix} \frac{d\mathbf{x}'^{(1)}}{d\beta}(\beta) \\ 0 \end{pmatrix} \times \begin{pmatrix} \mathbf{x}'^{(2)}(\beta) \\ 1 \end{pmatrix} + \begin{pmatrix} \mathbf{x}'^{(1)}(\beta) \\ 1 \end{pmatrix} \times \begin{pmatrix} \frac{d\mathbf{x}'^{(2)}}{d\beta}(\beta) \\ 0 \end{pmatrix} \quad (21)$$

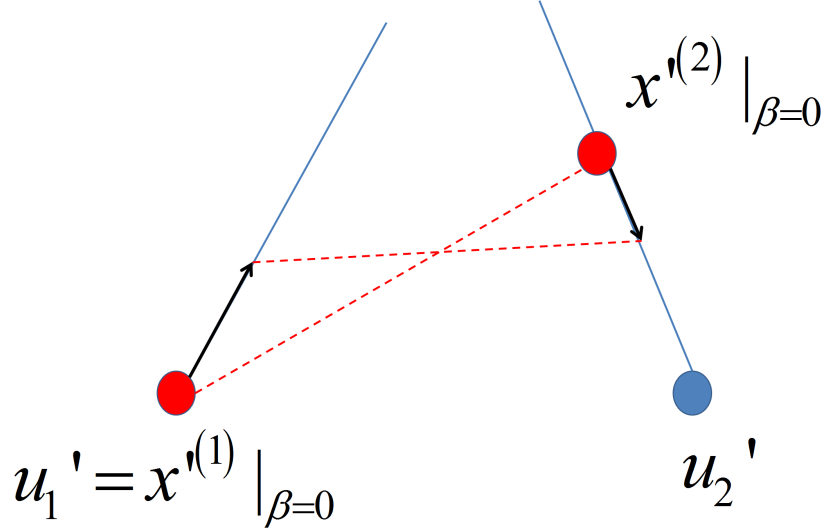


Figure 3: An illustration of epipolar constraints from two affine correspondences. The first linear constraint is formed by the line connecting the point $\mathbf{x}(\beta = 0)$ as seen by H_1 , $(\mathbf{x}'^{(1)}|_{\beta=0})$, and as seen by H_2 , $(\mathbf{x}'^{(2)}|_{\beta=0})$. A second constraint is formed by an infinitesimal movements of β around 0 as the line connecting $\mathbf{x}'^{(1)}|_{\beta=0+\epsilon}$ and $\mathbf{x}'^{(2)}|_{\beta=0+\epsilon}$.

If all the terms of (20) and (21) were known, then the epipole location could be determined as the intersection of the two lines. In the following derivation we evaluate (20) and (21) at $\beta = 0$; the quantities at $\beta = 0$ correspond to the transformations of \mathbf{u}_1 by the two homographies. The terms $\mathbf{x}'^{(1)}|_{\beta=0}$ and $\frac{d\mathbf{x}'^{(1)}}{d\beta}|_{\beta=0}$ can be expressed directly by the affine correspondence

$(\mathbf{u}_1, \mathbf{u}'_1, A_1)$ as:

$$\mathbf{x}'^{(1)}|_{\beta=0} = \mathbf{u}'_1 \quad (22)$$

$$\frac{d\mathbf{x}'^{(1)}}{d\beta}|_{\beta=0} = \mathbf{v}_1 \quad (23)$$

We therefore remain with two unknown terms $\frac{d\mathbf{x}'^{(2)}}{d\beta}|_{\beta=0}$ and $\mathbf{x}'^{(2)}|_{\beta=0}$. The remaining terms are calculated from the affine correspondence $(\mathbf{u}_2, \mathbf{u}'_2, A_2)$. Since the local derivatives of H_2 at \mathbf{u}_2 are known, the line connecting \mathbf{u}_1 and \mathbf{u}_2 is transferred by H_2 to the line that pass through \mathbf{u}'_2 in the direction of \mathbf{v}_2 . In Appendix A we show that given a parameterization to the line:

$$\mathbf{x}'^{(2)}(\beta') = \mathbf{u}'_2 + \beta' \mathbf{v}_2 \quad (24)$$

the relation between the parameterizations (19) and (24) is a one dimensional homography; we denote it as $t(\beta) = \beta' = \frac{(1+\beta)}{(1+\beta)(h_3, h_6)(\mathbf{u}_1 - \mathbf{u}_2) + 1}$. If the one dimensional homography, t , was known, we could easily extract the missing parameters for (20) and (21).

A one dimensional homography can be determined by two pairs of corresponding points and a derivative (see Appendix B). By the affine correspondence $(\mathbf{u}_2, \mathbf{u}'_2, A_2)$ we have from (A.3) that $t|_{\beta=-1} = 0$ and $\frac{dt}{d\beta}|_{\beta=-1} = 1$. In order to complete the puzzle, a single point correspondence on the line is still missing. However, as no more corresponding points along the line (24) are known, we set a parameter, α , that determines the location of the transformation of \mathbf{u}_1 by t . By defining the missing match as $\alpha = t|_{\beta=0}$ we have that

$$\mathbf{x}'^{(2)}|_{\beta=0} = \mathbf{u}'_2 + \alpha \mathbf{v}_2 \quad (25)$$

In Appendix B, we explicitly calculate the homography and show that $\frac{dt}{d\beta}|_{\beta=0} = \alpha^2$. A simple use of the derivatives chain rule then yields

$$\frac{d\mathbf{x}'^{(2)}}{d\beta}|_{\beta=0} = \alpha^2 \mathbf{v}_2 \quad (26)$$

Equations (22),(23),(25) and (26) determine all the terms of (20) and (21) at $\beta = 0$. We can therefore write the location of the epipole as

$$\begin{aligned} \mathbf{e} &= \mathbf{l}(0) \times \frac{d\mathbf{l}}{d\beta}(0) \\ &= \left(\left(\begin{pmatrix} \mathbf{u}'_1 \\ 1 \end{pmatrix} \times \begin{pmatrix} \mathbf{u}'_2 + \alpha \mathbf{v}_2 \\ 1 \end{pmatrix} \right) \right) \\ &\quad \times \left(\left(\begin{pmatrix} \mathbf{v}_1 \\ 0 \end{pmatrix} \times \begin{pmatrix} \mathbf{u}'_2 + \alpha \mathbf{v}_2 \\ 1 \end{pmatrix} \right) + \begin{pmatrix} \mathbf{u}'_1 \\ 1 \end{pmatrix} \times \begin{pmatrix} \alpha^2 \mathbf{v}_2 \\ 0 \end{pmatrix} \right) \end{aligned} \quad (27)$$

At a first glance, the curve may seem like a 3rd order rational curve. However, the third order term cancels out as a cross product of two vectors of the same direction. We show in Appendix C that the curve parameterization is equivalent to:

$$\mathbf{e} = \alpha^2 k_2 \begin{pmatrix} \mathbf{u}'_1 \\ 1 \end{pmatrix} + (\alpha \det(\mathbf{v}_1, \mathbf{v}_2) - k_1) \begin{pmatrix} \mathbf{u}'_2 + \alpha \mathbf{v}_2 \\ 1 \end{pmatrix} \quad (28)$$

where $k_i = \det(\mathbf{v}_i, \mathbf{u}'_1 - \mathbf{u}'_2)$. The epipole is therefore located on a second order rational curve - a conic parameterized by α . Note that we have only used partial information from the affine correspondence, as only the derivatives in the direction of the line connecting \mathbf{u}_1 and \mathbf{u}_2 were used for the calculation of the conic constraint.

3.1. Classification of the Conic

A classification of the conic (28) to an ellipse, hyperbola or parabola can be derived directly from the representation of the conic in non homogeneous coordinates:

$$\mathbf{e}_n = \frac{\alpha^2 k_2 \mathbf{u}'_1 + (\alpha \det(\mathbf{v}_1, \mathbf{v}_2) - k_1)(\mathbf{u}'_2 + \alpha \mathbf{v}_2)}{\alpha^2 k_2 + \alpha \det(\mathbf{v}_1, \mathbf{v}_2) - k_1} \quad (29)$$

The denominator of (29) is a second order polynomial with discriminant

$$\Delta = \det(\mathbf{v}_1, \mathbf{v}_2)^2 + k_1 k_2 \quad (30)$$

A second order curve can be classified by the number of its intersections with the point at infinity (which is equal to the number of the distinct roots of the denominator). The conic is therefore an hyperbola if the denominator of (29) has two distinct roots ($\Delta > 0$), a parabola in the case where the two roots are equal ($\Delta = 0$) and an ellipse is no roots exist ($\Delta < 0$).

3.2. Properties of the Conic

Some interesting properties of the conic constraints can be derived from (28). We next show that the conic passes through \mathbf{u}'_1 and \mathbf{u}'_2 and that the directions \mathbf{v}_1 and \mathbf{v}_2 are tangents to the curve at the point \mathbf{u}'_1 and \mathbf{u}'_2 respectively (see Figure 4).

The point \mathbf{u}'_2 is shown to be on the conic by setting $\alpha = 0$ in (29), hence $\mathbf{e}_n(0) = \mathbf{u}'_2$. Also $\mathbf{e}_n(\frac{k_1}{\det(\mathbf{v}_1, \mathbf{v}_2)}) = \mathbf{u}'_1$. The derivatives of the curve can be calculated from the inhomogeneous representation (29). By taking the derivatives of \mathbf{e}_n relative to α , one can easily show that $\frac{d\mathbf{e}_n}{d\alpha}(0) \cong \mathbf{v}_2$ and $\frac{d\mathbf{e}_n}{d\alpha}(\frac{k_1}{\det(\mathbf{v}_1, \mathbf{v}_2)}) \cong \mathbf{v}_1$ where the symbol \cong represent equality up to a scale factor.

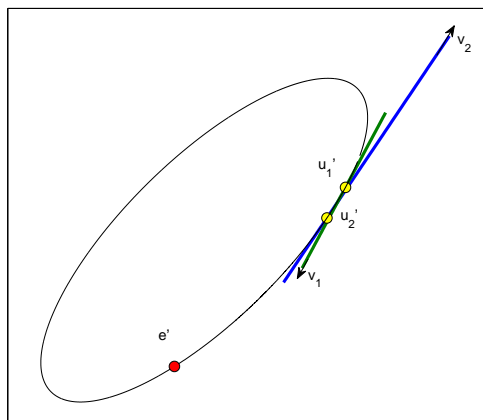


Figure 4: Conic constraint on the epipole generated from two affine correspondences. The green and blue lines mark the directions of \mathbf{v}_1 and \mathbf{v}_2 respectively. Note that the curve passes through \mathbf{u}'_1 and \mathbf{u}'_2 and is tangent to \mathbf{v}_1 and \mathbf{v}_2 . The epipole \mathbf{e}' is located on the conic constraint.

4. Experiments - Fundamental Matrix Calculation by Conic Intersections

In this section we describe experiments for calculating the fundamental matrix using conic constraints. Given three affine correspondences, each affine correspondence contributes a conic constraint on the location of the epipole. The epipole can therefore be located by intersection of conics; the fundamental matrix is then calculated from the affine correspondences and the known location of the epipole.

We perform two sets of experiments. In Section 4.2 we test the accuracy of the proposed method in a synthetic scenario: Three regions are placed on three planes viewed by 2 cameras. The measurements are then contaminated

with additive noise. We measure the accuracy of the proposed method, compared with the results of the normalized 8 points algorithm [17] on 3 points extracted from each region. In Section 4.3 we compare the proposed method with the point based method described in [11] for estimating the fundamental matrix from matching regions extracted by MSER [7]. We use both methods in a Locally Optimized RANSAC (LO-RANSAC) [16] robust estimation process. The compared methods are used for initial estimation of the fundamental matrix; each time the number of inliers is increased, the fundamental matrix is re-estimated from the new set of inliers, using the normalized 8 points algorithm on a larger number of regions. We measure the average number of iterations required by LO-RANSAC with each of the methods.

We first describe the method we use for calculating the fundamental matrix.

4.1. Calculation of the Fundamental Matrix from Affine Correspondences

Once the epipole location is known, we use the following method for calculating the fundamental matrix: Let H_1 be an homography and let $(\mathbf{u}_1, \mathbf{u}'_1, A_1)$ be an affine correspondence on the homography (the homography is not fully determined; the affine correspondence and the homography are related by (7)). Also let $(\mathbf{u}_2, \mathbf{u}'_2), (\mathbf{u}_3, \mathbf{u}'_3)$ be two additional correspondences *unrelated* to H_1 . We employ the point correspondences $(\mathbf{u}_2, \mathbf{u}'_2)$ and $(\mathbf{u}_3, \mathbf{u}'_3)$ to determine two additional constraints on H_1 and therefore fully determine H_1 .

Each additional point correspondence on H_1 is determined by the intersection of two lines. The first line is the transformation of the line connecting \mathbf{u}_1 to \mathbf{u}_2 by H_1 ; it is transformed to a line parameterized as $\mathbf{u}'_1 + \gamma A_1(\mathbf{u}_2 - \mathbf{u}_1)$. The second line is calculated by the epipolar geometry. According to the

epipolar geometry, \mathbf{u}_2 is transformed by H_1 to a location along the line connecting \mathbf{u}'_2 and the epipole e' (similarly to the scenario in Figure 2). The intersection of the lines yields an additional point correspondence on H_1 (see Figure 5); we denote it as $\mathbf{u}_2^{(1)}$. An additional point $\mathbf{u}_3^{(1)}$ is found by the same method applied to $(\mathbf{u}_3, \mathbf{u}'_3)$. Once the additional correspondences are calculated, the homography H_1 can be calculated from (7) using the constraints implied by the affine correspondence $(\mathbf{u}_1, \mathbf{u}'_1, A_1)$ and the two points of correspondence $(\mathbf{u}_2, \mathbf{u}_2^{(1)}), (\mathbf{u}_3, \mathbf{u}_3^{(1)})$. (Note that each of the point correspondences only contributes a single new constraint, as the direction of the transformation of the point by the homography relative to \mathbf{u}'_1 is already known from the affine correspondence). Since the fundamental matrix is directly determined by the epipole and an homography [2], we therefore have an alternative method to the normalized 8 points for calculation of the fundamental matrix F as $F = [\mathbf{e}']_x H_1$.

4.2. Comparison of the Conics Intersections Method with the Simulated Points Method

As mentioned above, most methods that do employ additional information from affine correspondences (such as [12] and [11]) do so by extracting additional point correspondences. A minimal number of 3 correspondences is required in order to represent the affine relation. Since an affine correspondence is only a local approximation of an homography, the simulated correspondence points are placed near the point of affine correspondence. We conducted a computer simulation to test the accuracy in calculating the fundamental matrix from points simulated by the affine transformation versus calculation from the conic constraints presented here.

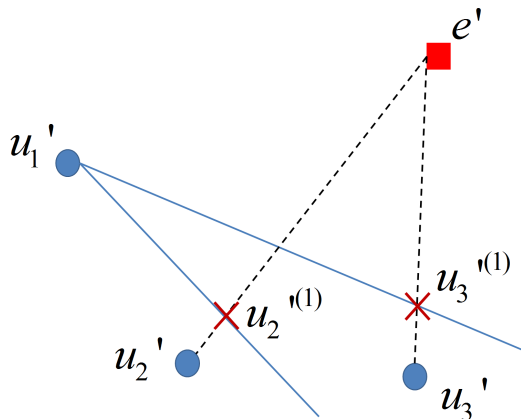


Figure 5: Additional correspondence points on an homography H_1 with a known affine correspondence $(\mathbf{u}_1, \mathbf{u}'_1, A_1)$. The correspondences, $\mathbf{u}_2'^{(1)}$ and $\mathbf{u}_3'^{(1)}$, are extracted by the intersection of epipolar lines and the transformation by H_1 of the lines that connect \mathbf{u}_1 to \mathbf{u}_2 and \mathbf{u}_1 to \mathbf{u}_3 . The epipolar lines are marked as dashed lines.

In the experiment, three groups of nearby points are viewed by two cameras. Each group consists of three points and is located on a different plane. The angle between the first two planes varies in the simulations, the third plane is perpendicular to the two other planes. The configuration is illustrated in Figure 6. A fundamental matrix is estimated once from the nine points of correspondence using the normalized eight points method and once from the epipole location and an affine correspondence as described above.

We measure the accuracy in the estimation of the fundamental matrix in the presence of noise. The location of each group of points is shifted by a white Gaussian noise. The locations within the groups are also shifted by noise, relative to the distance between the points in the groups. Let u_j^i be the j point of the group i . Also let ξ be the distance between the points in

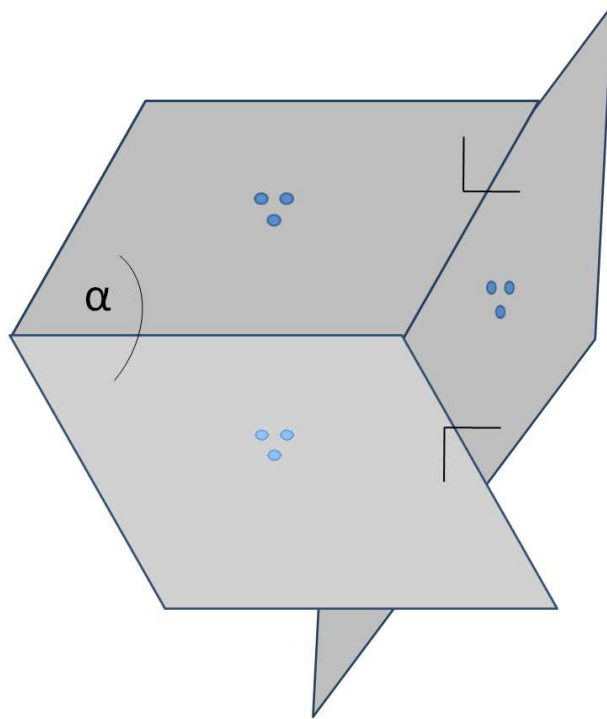


Figure 6: Three groups of three points used for comparison of direct calculation of the fundamental matrix with the proposed method. Each group is located on one plane. The angle between two of the planes is α . The fundamental matrix is calculated for two cameras viewing the configuration.

each group. The coordinates of each point are perturbed by noise so that

$$\tilde{\mathbf{u}}_j^i = \mathbf{u}_j^i + \gamma(\mathbf{n}^i + \xi\mathbf{n}_j^i) \quad (31)$$

where γ determines the magnitude of the noise and $\mathbf{n}^i, i = 1..3$, $\mathbf{n}_j^i, i = 1..3, j = 1..3$ are zero mean uncorrelated Gaussian random variables. The distance between the estimations of the fundamental matrix by each of the methods and the theoretical matrix is measured by normalizing each matrix to have a unit norm (since the matrices are only determined up to scale) and taking the Hilbert-Schmidt norm of the difference of the matrices. Our method produces up to 9 solutions (up to 12 intersections of the three conics where 3 of the intersections are located on the correspondence points) ; we therefore choose the fundamental matrix that minimizes the geometric distance between the 9 matched points and the corresponding epipolar lines by that fundamental matrix.

We conducted 1000 experiments for each value of γ . The proposed method provides higher accuracy than the calculation of the fundamental matrix by the normalized 8 points algorithm using the 9 point correspondences. The results for angles of $60^\circ, 120^\circ$ and 180° between the first two planes are presented in Figure 7. The results obtained by the proposed method are more accurate than the point based method. The improvement depends on the angle between the planes; the greatest improvement was measured in the two planes scenario (180° between the first and second plane) where it reached an order of magnitude. An example of the calculated epipole location and the conics is displayed in Figure 8.

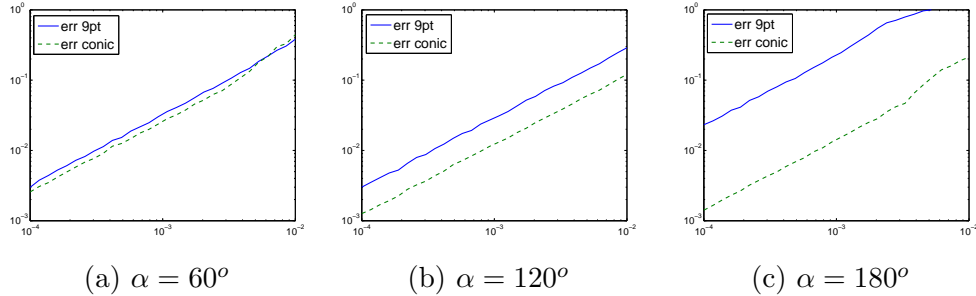


Figure 7: Estimation of the fundamental matrix by conic intersection and by using the normalized 8 points method from 9 points. The x axis represents the noise standard deviation (relative to the size of the region) and the y axis represents the error in the fundamental matrix (hilbert schmidt norm of matrices). The results are an average of 1000 experiments.

4.3. Matching with Low Inliers Rate

Calculation of the fundamental matrix requires correspondence of points or regions. In most cases, a correspondence between images is not known; only hypotheses for correspondences are known. A correct calculation of the fundamental matrix must rely only on correct hypotheses. The problem of separating the correct hypotheses (inliers) from the incorrect hypotheses (outliers) is usually tackled by robust statistical methods such as RANSAC[18].

In a RANSAC based solution, hypotheses are chosen at random and the fundamental matrix is calculated from the chosen hypotheses. The rest of the hypotheses are then used to vote for the correctness of the model. Since all hypotheses used for the calculation should be correct, the inliers rate and the number of hypotheses required for calculating the fundamental matrix greatly affect the number of attempts that should be done until a successful calculation is made. For example, point based methods that only employ the

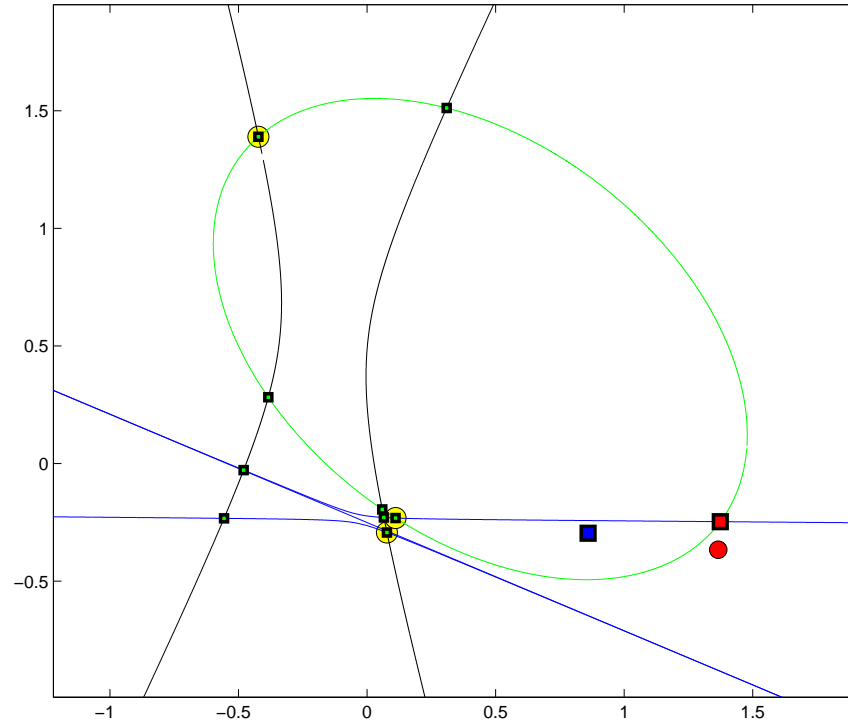


Figure 8: Calculation of the epipole by conic intersection and by the normalized 8 points method from a noisy observation. The yellow circles mark the location of the feature groups, the green rectangles mark intersection of conics, a red rectangle marks the intersection closest to the epipole (chosen as the intersection that minimizes the geometric distance of the points from the epipolar lines) and a blue rectangle marks the location of the epipole calculated by the normalized 8 points method. The true location of the epipole is marked by a red circle.

center of mass of the regions require a minimum of 7 points for calculation of the fundamental matrix; if the inliers rate is 10%, an average of 1×10^7 attempts are required for obtaining a successful guess. Therefore, such methods are only applicable when the inliers rate is high.

In this section we demonstrate the use of the epipolar conic constraint for calculating the fundamental matrix in the presence of low inliers rate. As the proposed method only relies on the correspondence of 3 regions, it is applicable to cases where the initial inliers rate is low. We compare the proposed method with [11]. The method presented in [11] also employs the affine approximation from the matched regions. It does so by representing each matched region by 3 points. Therefore, the fundamental matrix can be calculated from 3 corresponding regions (9 points).

As in [11], Locally Optimized RANSAC [16] is used for robust estimation of the fundamental matrix. In such an estimation scheme, in each iteration the model is calculated from 3 regions either by the proposed method or by [11]. If the number of inliers in the current iteration is higher than in all the previous iterations, the **local optimization** process is employed. The structure of the LO-RANSAC is described in Algorithm 1.

The local optimization is performed in an iterative manner. In each iteration of the local optimization, a new model is calculated by performing RANSAC on all matched regions with error (distance of the center of mass of the regions from the corresponding epipolar line) lower than $K \cdot \theta$ from the previous model. The value of K is decreased until the final model is calculated for $K = 1$. Since the inlier rate is high in this phase (we start from the initial model calculated from the 3 regions), we use more than 3

Repeat until the probability of missing a set of inliers falls under a predefined threshold (As in standard RANSAC)

1. Select a random sample of 3 matched regions and calculate the fundamental matrix from the regions.
2. Calculate the number of inliers I_k , i.e., the data points their error is smaller than predefined threshold θ .
3. if a new maximum of inliers has occurred ($I_k > I_j$ for all $j < k$), run **local optimization** and store the best model.

Algorithm 1: A general scheme of a LO-RANSAC robust estimation.

regions for the calculation. As advised in [16], $\min(I_k/2, 14)$ matches are used for calculating the fundamental matrix using the normalized 8 points algorithm. For compatibility with the experiment in [11], only the center of mass of the regions is used for the local optimization.

We use the Daisy dataset [19],[20] and the Leuven city hall dataset [21],[22] to compare the performance of the methods. The Daisy dataset contains 4 pairs of images. The Leuven city hall dataset contains a sequence of 6 images; we calculate the epipolar geometry of the first image with any other image.

We extracted MSER [7] regions from each image. Given a region $\Omega \in R^2$ with a center of mass at $\boldsymbol{\mu}$, it is shown in [10] that a coordinate system, $\mathbf{u}^{(n)}$, invariant to affine transformations, can be determined from the second order

Image pair	#Hypotheses	#Inliers Rate	#Conic Iterations	#3 Points Iterations
daisy1	313	16.3 %	1566	1627
daisy2	365	22.5 %	497	504
daisy3	378	14.3 %	2376	2462
daisy4	260	14.6 %	2348	2456
leuven2	2448	68.8 %	13	13
leuven3	1521	45.0 %	51	52
leuven4	1053	23.7 %	381	386
leuven5	986	12.4 %	2700	2720
leuven6	945	9.4 %	7209	7585

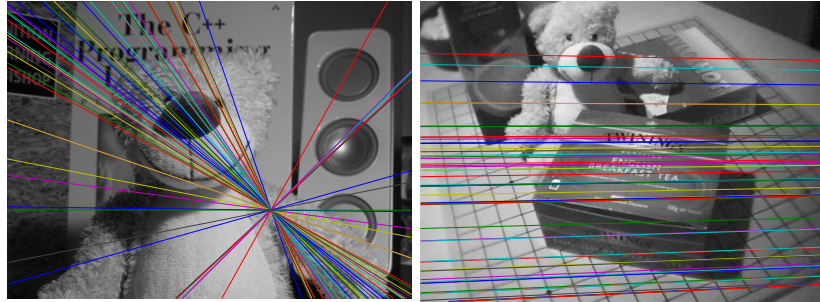
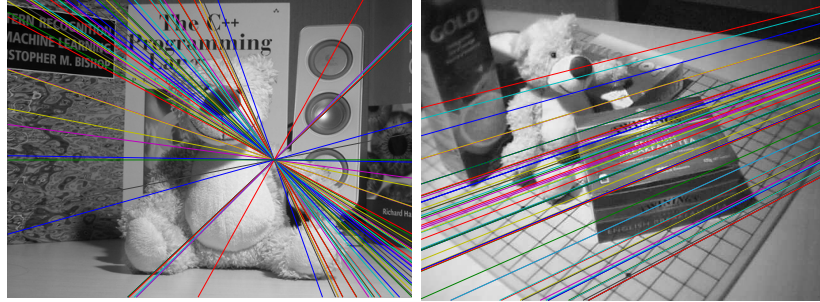
Table 1: Mean number of LO-RANSAC iterations using the proposed (conic) method and by extraction of 3 points from each region.

moment matrix of the region, such that

$$\mathbf{u}^{(n)} = RM^{-\frac{1}{2}}\mathbf{u} \quad (32)$$

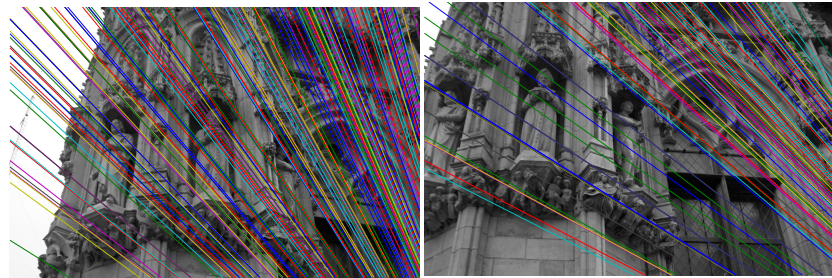
where R is an unknown rotation matrix and $M = \frac{1}{|\Omega|} \int_{\Omega} (\mathbf{x} - \boldsymbol{\mu})(\mathbf{x} - \boldsymbol{\mu})^T d\mathbf{x}$. We use the SIFT descriptor [23] both to detect the unknown rotation (by the dominant gradient location of the image at Ω) and to describe the image in the affine normalized coordinates system. We then create match hypotheses by the similarity of the SIFT descriptor.

The affine normalization of the regions is also used to determine an affine transformation for each match hypotheses (for the proposed method) and to determine 3 points of correspondence (for [11]). The first point is the center of mass of the matched regions, two additional points of correspondence are the transformations of unit vectors in the directions of the x axis and the y



(a) daisy 1, 16.3 % inliers

(b) daisy 3, 14.3 % inliers



(c) leuven 4, 12.4 % inliers

(d) leuven 6, 9.4 % inliers

Figure 9: Calculated epipolar lines of pairs with low inliers rate using the proposed method.

axis in the normalized coordinate systems to the coordinate systems of the images.

We perform 100 experiments for each pair of images and measure the average number of iterations required by the LO-RANSAC algorithm. The results are summarized in Table 1; examples of the pairs of images with epipolar lines calculated using the proposed method are shown in Figure 9. The proposed method produces comparable and slightly better results than the state of the art, point based, method. Note that in this experiment the methods are not compared directly as an additional phase of estimation from more than three points is needed. Hence, the improvement over the point based method is not as big as in the synthetic experiment. The additional phase is required as the affine relations are not estimated with sufficient accuracy. Thus, comparison of the results of the synthetic experiment, to those obtained on real data leads to the conclusion that higher precision in estimating the local affine features is essential in order to achieve the potential performance gain of the proposed method, over the point the based method. Since the parameters of the local affine features are estimated by the MSER based procedure with only a limited accuracy, both the proposed method and the point based method can only serve as initializers in a Lo-RANSAC framework, and both provide comparable performance in this task. We are currently investigating new methodologies for improving the accuracy in estimating the parameters of local affine models from small image patches.

5. Conclusion

Although affine correspondences are widely used for obtaining matches between images, a comprehensive analysis of the constraints on epipolar geometry from affine correspondences has not been previously conducted. This paper provides a detailed analysis of the problem.

We have proved that each affine correspondence yields 3 linear constraints on the fundamental matrix. Furthermore, if the linear constraints are satisfied, the affine correspondence can be completed to an homography. By using the homography structure it is shown that although two affine correspondences do not fully determine the fundamental matrix, they constrain the location of the epipole to a conic. A simple parameterization of the conic by the affine correspondences was derived along with the properties of the conic. This further demonstrates that an affine correspondence is not equivalent to a 3 point correspondence, as in the case of 6 corresponding points (3 from each affine correspondence) it was shown by Faugeras [5] that the epipole is constrained to a cubic instead of a conic.

The conic constraint on the epipole was employed for calculation of the fundamental matrix from 3 affine correspondences. Experiments on synthetic data show that the calculation by intersection of conics is more accurate than the direct calculation by using the normalized 8 points method on points simulated from the affine correspondences. We further showed that since only 3 regions are required for calculating the fundamental matrix, the proposed method can be used for matching in scenarios where the inlier rate is low. However, as current affine estimation methods from small image patches are not accurate enough to enable accurate estimation of the fundamental

matrix, on real data both the proposed and the simulated data methods can only serve as initializers for point based estimation from a larger number of points. Thus, comparison of the results of the synthetic experiments, to those obtained on real data leads to the conclusion that higher precision in estimating the local affine features is essential in order to achieve the potential performance gain of the proposed method, over the point the based methods.

Appendix A. One Dimensional Homography Between Line Parameterizations

We show here that the relation between the line parameterization β and β' in (19) and (24) is a one dimensional homography. As shown in (7) H_2 can be represented as

$$H_2 = S_{u'_2} \begin{pmatrix} a_1 & a_3 & 0 \\ a_2 & a_4 & 0 \\ h_3 & h_6 & 1 \end{pmatrix} S_{-u_2} \quad (\text{A.1})$$

where a_1, \dots, a_4 denote the terms of A_2 . The image of a point $x(\beta) = \mathbf{u}_1 + \beta(\mathbf{u}_1 - \mathbf{u}_2)$ by the homography H_2 is

$$H_2 \begin{pmatrix} x(\beta) \\ 1 \end{pmatrix} = S_{u'_2} \begin{pmatrix} a_1 & a_3 & 0 \\ a_2 & a_4 & 0 \\ h_3 & h_6 & 1 \end{pmatrix} \begin{pmatrix} (1 + \beta)(u_1 - u_2) \\ 1 \end{pmatrix} \quad (\text{A.2})$$

Recalling that $\mathbf{v}_2 = A_2(\mathbf{u}_1 - \mathbf{u}_2)$ we can rewrite (A.2) by treating (h_3, h_6) as a 2D vector as

$$S_{\mathbf{u}'_2} \begin{pmatrix} (1 + \beta)\mathbf{v}_2 \\ (1 + \beta)(h_3, h_6)(\mathbf{u}_1 - \mathbf{u}_2) + 1 \end{pmatrix} \cong \begin{pmatrix} \mathbf{u}'_2 + \frac{(1+\beta)}{(1+\beta)(h_3, h_6)(\mathbf{u}_1 - \mathbf{u}_2) + 1} \mathbf{v}_2 \\ 1 \end{pmatrix} \quad (\text{A.3})$$

where \cong represents equality up to a scale factor. The relation between β to β' is therefore a one dimensional homography.

Appendix B. One Dimensional Homography Calculation from Derivative and Points

We next show that a one dimensional homography can be calculated from 2 points and a derivative: A general form of a 1-D homography is given by

$$\beta' = \frac{a\beta + b}{c\beta + 1} \quad (\text{B.1})$$

If $\beta' = 0$ corresponds to $\beta = 0$, then $b = 0$ and $\frac{d\beta'}{d\beta}|_{\beta=0} = a$. In the general case, where β_0 correspond to some β'_0 and the derivative at β_0 is $\frac{d\beta'}{d\beta}|_{\beta=\beta_0} = a$, we can express the one dimensional homography in homogeneous coordinates as

$$t = \begin{pmatrix} 1 & \beta'_0 \\ 0 & 1 \end{pmatrix} \begin{pmatrix} a & 0 \\ c & 1 \end{pmatrix} \begin{pmatrix} 1 & -\beta_0 \\ 0 & 1 \end{pmatrix} \quad (\text{B.2})$$

In section 3, two parameterizations of a corresponding line by the homography H_2 are given by (19) and (24). By the affine correspondence $(\mathbf{u}_2, \mathbf{u}'_2, A_2)$ we have that $\beta'(\beta = -1) = t|_{\beta=-1} = 0$ and $\frac{dt}{d\beta}|_{\beta=-1} = 1$. Substituting into the general homography (B.2), the homography t is therefore given by

$$t = \begin{pmatrix} 1 & 0 \\ 0 & 1 \end{pmatrix} \begin{pmatrix} 1 & 0 \\ c & 1 \end{pmatrix} \begin{pmatrix} 1 & 1 \\ 0 & 1 \end{pmatrix} = \begin{pmatrix} 1 & 1 \\ c & c+1 \end{pmatrix} \quad (\text{B.3})$$

where c is yet to be determined. By the chosen parameterization $t|_{\beta=0} = \alpha$, hence $c = \frac{1}{\alpha} - 1$. Since the homography is now fully parameterized by α , we can compute the derivative of t at $\beta = 0$; we therefore have that $\frac{dt}{d\beta}|_{\beta=0} = \alpha^2$.

Appendix C. Curve Reparameterization

Let $\mathbf{a}, \mathbf{b}, \mathbf{c}, \mathbf{d}$ be some known vectors in R^3 , where $\mathbf{e} = (\mathbf{a} \times \mathbf{b}) \times ((\mathbf{c} \times \mathbf{b}) + (\mathbf{a} \times \mathbf{d}))$. A reformulation of \mathbf{e} can be written as

$$\mathbf{e} = (\mathbf{a} \times \mathbf{b}) \times (\mathbf{a} \times \mathbf{d}) + (\mathbf{b} \times \mathbf{a}) \times (\mathbf{b} \times \mathbf{c}) = [\mathbf{a} \cdot (\mathbf{b} \times \mathbf{d})] \mathbf{a} + [\mathbf{b} \cdot (\mathbf{a} \times \mathbf{c})] \mathbf{b} \quad (\text{C.1})$$

We can use the formulation to rewrite equation (27): Let $\mathbf{a} = \begin{pmatrix} \mathbf{u}'_1 \\ 1 \end{pmatrix}$,

$\mathbf{b} = \begin{pmatrix} \mathbf{u}'_2 + \alpha \mathbf{v}_2 \\ 1 \end{pmatrix}$, $c = \begin{pmatrix} \mathbf{v}_1 \\ 0 \end{pmatrix}$ and $\mathbf{d} = \begin{pmatrix} \alpha^2 \mathbf{v}_2 \\ 0 \end{pmatrix}$, the term $\mathbf{b} \times \mathbf{d}$ is rewritten as

$$(\mathbf{b} \times \mathbf{d}) = \left(\begin{pmatrix} \mathbf{u}'_2 \\ 1 \end{pmatrix} + \alpha \begin{pmatrix} \mathbf{v}_2 \\ 0 \end{pmatrix} \right) \times \alpha^2 \begin{pmatrix} \mathbf{v}_2 \\ 0 \end{pmatrix} = \alpha^2 \begin{pmatrix} \mathbf{u}'_2 \\ 1 \end{pmatrix} \times \begin{pmatrix} \mathbf{v}_2 \\ 0 \end{pmatrix} \quad (\text{C.2})$$

Thus the term that multiply α^3 in (27) cancels out. Moreover, since $\mathbf{a} \cdot (\mathbf{b} \times \mathbf{d}) = \det(\mathbf{a}, \mathbf{b}, \mathbf{d}) = \alpha^2 k_2$ and $\mathbf{b} \cdot (\mathbf{a} \times \mathbf{c}) = \det(\mathbf{b}, \mathbf{a}, \mathbf{c}) = \alpha \det(\mathbf{v}_1, \mathbf{v}_2) - k_1$ then equation (27) can be written more compactly as

$$\mathbf{e} = \alpha^2 k_2 \begin{pmatrix} \mathbf{u}'_1 \\ 1 \end{pmatrix} + (\alpha \det(\mathbf{v}_1, \mathbf{v}_2) - k_1) \begin{pmatrix} \mathbf{u}'_2 + \alpha \mathbf{v}_2 \\ 1 \end{pmatrix} \quad (\text{C.3})$$

- [1] Q.-T. Luong, O. Faugeras, The fundamental matrix: Theory, algorithms, and stability analysis, *International Journal of Computer Vision* 17 (1) (1996) 43–75.
- [2] R. Hartley, A. Zisserman, *Multiple View Geometry in Computer Vision*, 2nd Edition, Cambridge University Press, New York, NY, USA, 2003.

- [3] Z. Zhang, Determining the epipolar geometry and its uncertainty: A review, *International Journal of Computer Vision* 27 (2) (1998) 161–195.
- [4] H. C. Longuet-Higgins, A computer algorithm for reconstructing a scene from two projections, *Nature* 293 (5828) (1981) 133–135.
- [5] O. Faugeras, *Three-dimensional computer vision: a geometric viewpoint*, MIT Press, Cambridge, MA, USA, 1993.
- [6] K. Mikolajczyk, C. Schmid, Scale & affine invariant interest point detectors, *International Journal of Computer Vision* 60 (1) (2004) 63–86.
- [7] J. Matas, O. Chum, M. Urban, T. Pajdla, Robust wide-baseline stereo from maximally stable extremal regions, *Image and Vision Computing* 22 (10) (2004) 761–767.
- [8] T. Tuytelaars, L. Van Gool, Matching widely separated views based on affine invariant regions, *International Journal of Computer Vision* 59 (1) (2004) 61–85.
- [9] T. Kadir, A. Zisserman, M. Brady, An affine invariant salient region detector, *Computer Vision - ECCV 2004* 3021 (2004) 228–241.
- [10] K. Mikolajczyk, T. Tuytelaars, C. Schmid, A. Zisserman, J. Matas, F. Schaffalitzky, T. Kadir, L. V. Gool, A comparison of affine region detectors, *International Journal of Computer Vision* 65 (2005) 2005.
- [11] O. Chum, J. Matas, S. Obdrzalek, Epipolar geometry from three corre-

- spondences, Computer Vision CVWW'03: Proceedings of the 8th Computer Vision Winter Workshop (2003) 83–88.
- [12] F. Riggi, M. Toews, T. Arbel, Fundamental matrix estimation via tip - transfer of invariant parameters, in: Proceedings of the 18th International Conference on Pattern Recognition - Volume 02, ICPR '06, IEEE Computer Society, Washington, DC, USA, 2006, pp. 21–24.
- [13] R. Szeliski, P. Torr, Geometrically constrained structure from motion: Points on planes, in: R. Koch, L. Gool (Eds.), 3D Structure from Multiple Images of Large-Scale Environments, Vol. 1506 of Lecture Notes in Computer Science, Springer Berlin Heidelberg, 1998, pp. 171–186.
- [14] M. Perdoch, J. Matas, O. Chum, Epipolar geometry from two correspondences, in: Proceedings of the 18th International Conference on Pattern Recognition - Volume 04, ICPR '06, IEEE Computer Society, Washington, DC, USA, 2006, pp. 215–219.
- [15] R. Arandjelovic, A. Zisserman, Efficient image retrieval for 3d structures, in: Proceedings of the British Machine Vision Conference, BMVA Press, 2010, pp. 30.1–30.11.
- [16] O. Chum, J. Matas, J. Kittler, Locally optimized ransac, in: B. Michaelis, G. Krell (Eds.), Pattern Recognition, Vol. 2781 of Lecture Notes in Computer Science, Springer Berlin Heidelberg, 2003, pp. 236–243.
- [17] R. I. Hartley, In defence of the 8-point algorithm, in: Proceedings of the

Fifth International Conference on Computer Vision, ICCV '95, IEEE Computer Society, Washington, DC, USA, 1995, pp. 1064–.

- [18] P. H. S. Torr, D. W. Murray, The development and comparison of robust methods for estimating the fundamental matrix, *International Journal of Computer Vision* 24 (1997) 271–300.
- [19] E. Tola, V. Lepetit, P. Fua, A fast local descriptor for dense matching, in: *Computer Vision and Pattern Recognition, 2008. CVPR 2008. IEEE Conference on*, 2008, pp. 1–8.
- [20] E. Tola, V. Lepetit, P. Fua, Daisy: An efficient dense descriptor applied to wide-baseline stereo, *Pattern Analysis and Machine Intelligence, IEEE Transactions on* 32 (5) (2010) 815 –830.
- [21] C. Strecha, R. Fransens, L. Van Gool, Combined depth and outlier estimation in multi-view stereo, in: *Computer Vision and Pattern Recognition, 2006. CVPR 2006. Proceedings of the 2006 IEEE Computer Society Conference on*, Vol. 2, 2006, pp. 2394–2401.
- [22] C. Strecha, R. Fransens, L. Van Gool, Wide-baseline stereo from multiple views: A probabilistic account, in: *Computer Vision and Pattern Recognition, 2004. CVPR 2004. Proceedings of the 2004 IEEE Computer Society Conference on*, Vol. 1, 2004, pp. 552–559.
- [23] D. Lowe, Distinctive image features from scale-invariant keypoints, *International Journal of Computer Vision* 60 (2) (2004) 91–110.